Experimental Verification of N-phase Inverter Connected to Multiple Coils for Dynamic Wireless Power Transfer

Chonghao Hong[*a)] Student Member, Osamu Shimizu[*] Member
Sakahisa Nagai[*] Member, Toshiyuki Fujita[*] Member
Hiroshi Fujimoto[*] Senior Member

Dynamic Wireless Power Transfer (DWPT) systems can extend cruising range and reduce the capacity of the battery of electric vehicles. The third-generation wireless in-wheel motor (W-IWM3), which has DWPT system, is one of the key specifications of electric vehicles. W-IWM3 adopts the DWPT system with one full-bridge inverter that operates only one coil. This paper discusses a N-phase inverter configuration and the switching algorithm that can independently operate multiple coils in the DWPT system. With this system, it is possible to control multiple coils with only one circuit configuration and reduce the number of inverter elements and inverter installations used on the roadside. The fundamental operation of the system was verified by simulation and experiment.

Keywords: dynamic wireless power transfer, magnetic resonance coupling, wireless in-wheel motor, electric vehicle

1. Introduction

In recent years, each country's interest in environmental issues including global warming has increased, and various policies have been implemented. Among them, electric vehicles (EVs), which can contribute to the reduction of greenhouse gases containing carbon dioxide, are attracting a great deal of attention. However, EVs, which have advantages such as being eco-friendly and having high controllability, are not as widespread as expected at present. The major reasons are short cruising range and long charging time.

A dynamic wireless power transfer (DWPT) system is one of the effective solutions because it can transfer electric power to moving EVs [1] [2]. DWPT is to receive power wirelessly from a transmitter coil installed on the road-side with a power receiver coil attached to EV-side. As a result, it can be charged without human intervention, and only the minimum required battery needs to be installed. Among them, the magnetic field resonance coupling method [3] is characterized by high efficiency and high power transmission even with a large air gap and wide misalignment [4]. It is expected as a technology suitable for supplying power to EVs while driving.

Vehicle system of EVs includes an onboard motor system or an in-wheel motor (IWM) system. In IWM, by installing the motor inside the wheels, each wheel is controlled independently to improve the motion control performance and cruising range. Therefore, our research group has proposed a new method of DWPT suitable for IWM-type EVs. Previous DWPT studies have mainly assumed that onboard motor-type EVs [5] [6]. In their studies, in-vehicle batteries are charged via a coil attached to the bottom of the vehicle. After that, the battery sends power to the motor to drive the EV. Instead of transferring electric power from the road coil to the vehicle coil to charge the battery, our proposed method is to transfer electric power directly from the road coil to the IWM while driving. In order to verify this concept with an actual vehicle, we have developed the second-generation wireless in-wheel motor (W-IWM2) equipped with a DWPT for traveling vehicles. In addition, the third-generation wireless in-wheel motor (W-IWM3) shown as Fig. 1 has been proposed [7]. W-IWM3 has improved WPT power, motor output, and size.

Fig. 1. The third generation wireless in-wheel motor.

Since the W-IWM3 uses SS-topology magnetic resonance coupling, one full-bridge inverter was required to operate one

a) Correspondence to: koh.chouhou19@ae.k.u-tokyo.ac.jp
[*] The University of Tokyo
5-1-5, Kashiwanoha, Kashiwa, Chiba, 227-8561 Japan
Phone: +81-4-7136-3881
Fax: +81-4-7136-3881

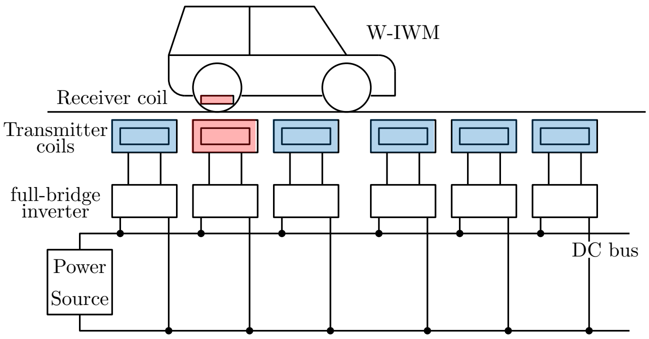

(a) The WPT system of W-IWM3 (basic system).

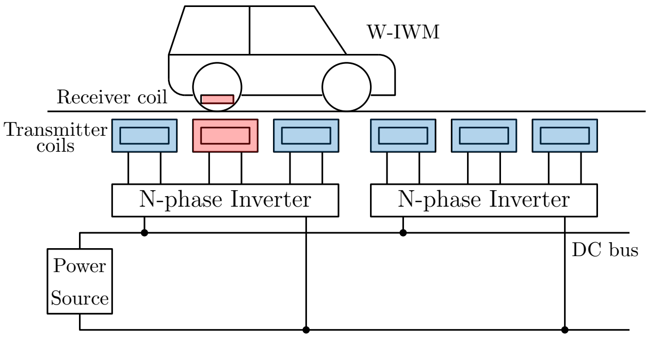

(b) The coil switching system with N-phase inverter (switching system).

Fig. 2. The concept of the coil switching system.

coil basically. However, if the number of installed coils is increased in order to lengthen the power supply time of the coils, the number of inverters will increase and the equipment cost will increase. Therefore, it is desirable to use one inverter to power multiple coils. Regarding previous research on coil switching, research on circuit configurations such as the method in which very long cables are installed along the traveling direction of an automobile and driven by a multi-phase inverter [8], and the method in which additional inductance and capacitors are incorporated into the circuit configuration [9].

This paper discusses the coil switching system with a N-phase inverter configuration and the control method that can independently drive multiple coils in the DWPT system. With the coil switching system, it is possible to control multiple coils with only one circuit configuration, and reduce the number of inverter elements and inverter installations used on the road side, making it possible to cut the cost of the DWPT system.

2. Switching system with a N-phase inverter

The concept is shown in Fig. 2. In this paper, the coil switching system is verified through experiments and simulations. Also, compare with the basic system, the paper discusses if there is any influence on basic operation in the switching system.

2.1 Basic WPT SS-topology The WPT system for W-IWM3 adopts SS-type magnetic resonance coupling WPT. Fig. 3 shows a general system configuration. On the road side of the WPT network, a full-bridge inverter converts DC current into AC current. The inverter on the transmitter side is mainly operated by PWM control. In the SS-type magnetic resonance coupling WPT, when the transmitter side and the

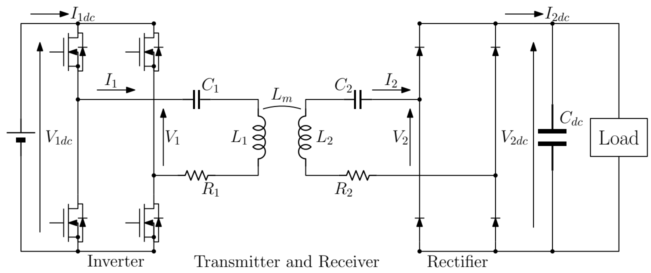

Fig. 3. Circuit configuration of SS-topology wireless power transfer.

Table 1. Comparison of system characteristic with $n-1$ transmitter coils

	Basic system	Switching system
Inverter	full-bridge inverter	N-phase inverter
Number of inverter	$n-1$	1
Number of legs	$2(n-1)$	n

receiver side satisfy the resonance condition, the operating angular frequency in the power conversion circuit can be expressed as follows [10].

$$\omega_0 = 2\pi f_0 = \frac{1}{\sqrt{L_1 C_1}} = \frac{1}{\sqrt{L_2 C_2}} \cdots\cdots (1)$$

Here, f_0 represents the resonance frequency. Also, the current flowing through the coil is

$$I_1 = \frac{R_2 V_1 + \omega_0 L_m V_2}{R_1 R_2 + (\omega_0 L_m)^2} \cdots\cdots (2)$$

$$I_2 = \frac{-R_1 V_2 + \omega_0 L_m V_1}{R_1 R_2 + (\omega_0 L_m)^2} \cdots\cdots (3)$$

$$k = \frac{L_m}{\sqrt{L_1 L_2}} \cdots\cdots (4)$$

$L_i (i = 1, 2)$ represents the self inductance of the transmitter and receiver coil. L_m represents the mutual inductance of the transmitter and receiver coil, and $R_i (i = 1, 2)$ represent the resistance of the transmitter and receiver coil, respectively. Also, $V_i (i = 1, 2)$ are discussed as the basic effective values in the operating frequency. Here, the subscript 1 represents the transmitter side and 2 represents the receiver side.

2.2 Circuit configuration The circuit configuration using a N-phase inverter for coil switching is shown in Fig. 4. Each transmitter coil is connected between each phase of a N-phase inverter. $n-1$ transmitter coils can be driven independently by the N-phase inverter. The most advantage of driving multiple coils using a N-phase inverter is the reduction of the transmission equipment cost and maintainability. The number of elements can be reduced compared to the configuration with the basic system. Reducing the number of independent inverters as much as possible and increasing the number of coils that can be controlled also leads to the reduction of the transmission equipment system cost. Hereinafter, the system with a full-bridge inverter is referred to as the basic system ,and the system with a N-phase inverter is referred to as the switching system. The features of those systems are summarized in Table 1.

The transmitter coils are connected between the two legs,

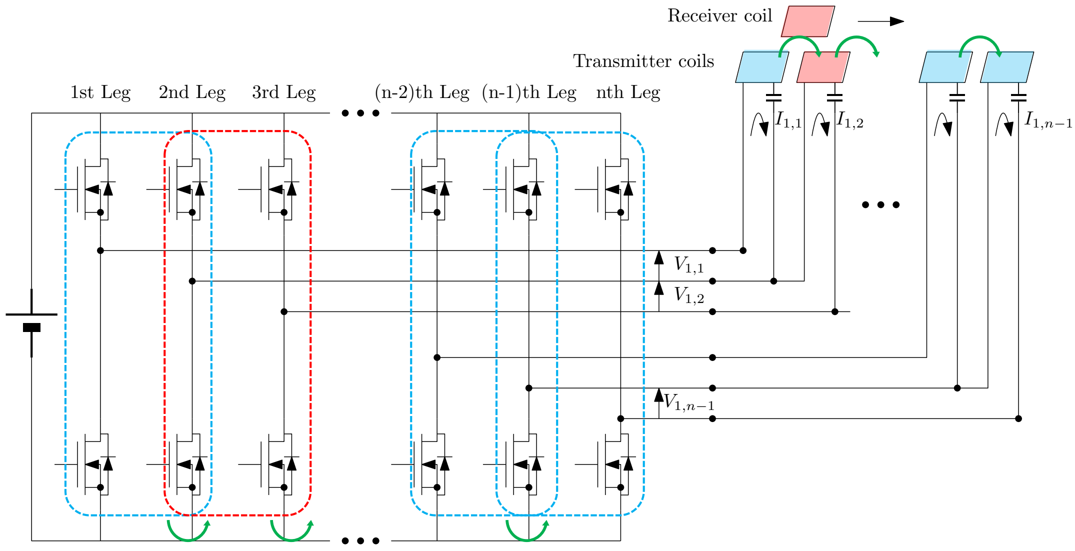

Fig. 4. Circuit configuration of the coil switching system with a N-phase inverter.

and each leg is shared by the two transmitter coils. For example, the 1_{st} transmitter coil is connected to the 1_{st} and 2_{nd} leg. When you want to operate the 1_{st} transmitter coil, the switching elements of the 1_{st} and 2_{nd} leg can be used. the 2_{nd} transmitter coil is connected to the 2_{nd} and 3_{rd} leg. The way to drive the 2_{nd} transmitter coil is the same as the 1_{st} transmitter coil. At that time, all other arms are in the gate-off state. As in Fig. 4, the transmitter coil is switched by shifting the leg connected to it in the power transmission section according to the movement of the receiver coil.

2.3 Switching algorithm Fig. 5 shows a flowchart of the power transmission procedure. As shown in Fig. 6, the mutual inductance between a transmitter coil and reciever coil is not constant in the longitudinal direction, and it becomes extremely smaller at the end of the coil than at the center. Therefore, if power is transmitted in a situation where the mutual inductance is quite small, a large current will flow, leading to equipment failure. It is necessary to stop power transmission at a certain place and wait until it moves to the next coil.

In this paper, the current threshold value I_{1th} is set in advance, and if the primary side current $I_{1,n}$ of the nth coil obtained by the current sensor exceeds that threshold value, it is judged that the power supply is completed in the section of the nth transmittercoil. After that, the nth full-bridge section stop PWM control. I_{1th} is determined by the rated value of the equipment, the power transmission stop point, and so on. As discussed in [6], (2) and (3) are equations in the steady state, but since the term of change in mutual inductance due to the movement of the receiver coil can be underestimated, they can also be used in DWPT.

Regarding vehicle detection and power transmission start time, the method discussed in [11] and the method using sensors can be considered, but this time this paper discusses the fundamental operation of coil switching, so it is assumed that the timing of power transmission start is known. That is, when starting to drive the next coil, it is assumed that the infomation of the speed of vehicle and the burial interval of transmitter coils are obtained. During the time calculated from that, the inverter will stop. After stopping for a certain

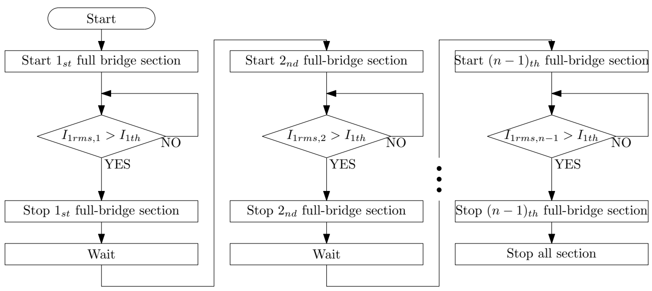

Fig. 5. Flowchart of coil switching.

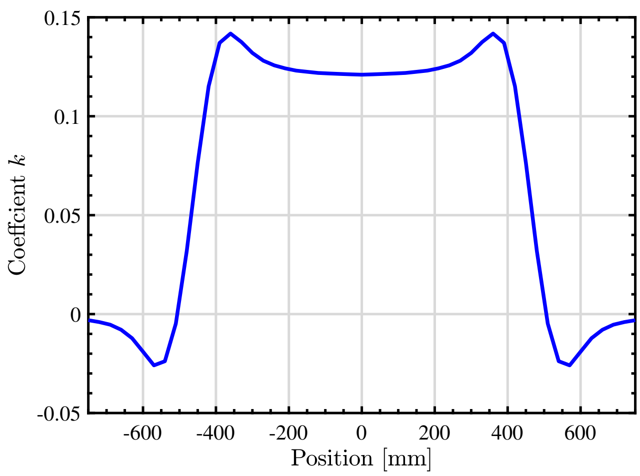

Fig. 6. Coupling coefficient with respect to the position of the receiver coil.

period of time, the next transmitter coil to which the vehicle body has moved starts to move in the same way. At this time, the drive of the next transmitter coil start from the point where the receiver coil, which is a point where the mutual inductance is sufficiently large, completely penetrates into the transmitter coil section.

3. Experiment and factor analysis

The feasibility of driving multiple coils using a N-phase inverter was verified by simulation and experiment. The simu-

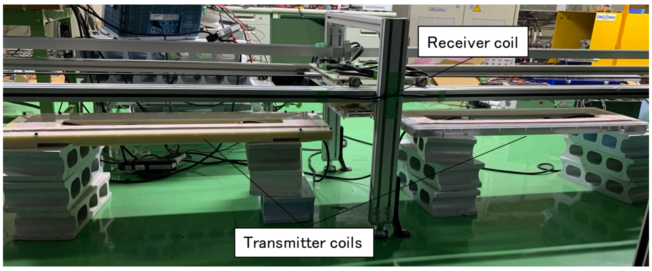

(a) Dynamic WPT bench.

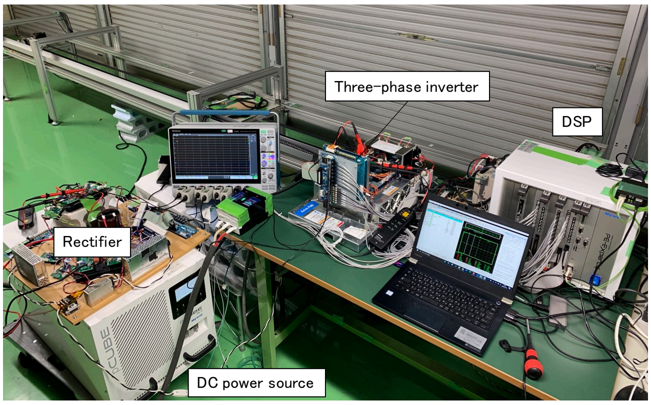

(b) Experimental set up.

Fig. 7. Equipments of dynamic WPT bench.

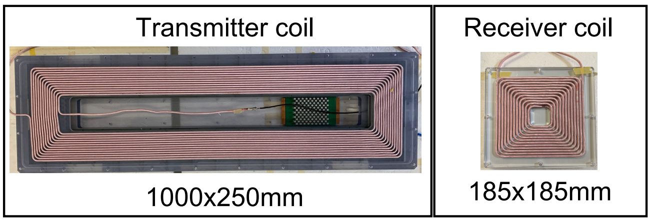

Fig. 8. Transmitter and receiver coil of W-IWM3

Table 2. Simulational and experimental condition of static situation.

Input voltage V_{1dc}	30 V
Output voltage V_{2dc}	30 V
frequency f_0	85.0 kHz

Table 3. Specification of coils.

	Transmitter coil(TX1)	Transmitter coil(TX2)	Receiver coil
Size of coil	1000x250 mm	1000x250 mm	185x185 mm
Resistance R	159.17 mΩ	223.15 mΩ	28.07 mΩ
Self inductance L	238.05 µH	244.91 µH	101.45 µH

lation was implemented and analyzed in MATLAB/Simulink. The experiment was performed on the bench imitating DWPT as shown in Fig. 7. The coils used in W-IWM3 are shown in Fig. 8. In this simulation and experiment, for the sake of simplicity, it is assumed that two transmitter coils are driven using a three-phase inverter. The values and coil parameters shown in Table 2 and Table 3 are used In the simulations and experiments.

3.1 Experimental results of static situaiton In order to confirm the fundamental operation, the experiment in static situation was conducted. The experiment is conducted under the conditions as assumed in Table 2, and the waveform at that time is shown in Fig. 9. In this experiment, the receiver coil(RX) is always one of the transmitter coils (TX1), and the mutual inductance is 23.5 µH. However, it can be seen that a voltage surge and a minute current are flowing in another of the transmitter coils (TX2) for a very short time. It is considered that the waveform is due to the parasitic capacitance provided in the switching elements under gate-off.

In order to consider how much the voltage and current in this TX2 affect the system, DC input and output power was measured in both the swithing system and the basic system. The result is shown in Fig. 10. Compared in terms of the effciency, the efficiency of the basic system was 87.4 %, and that of the switching system was 87.2 %. As shown in Fig. 10, it was found that the voltage and current were so small that they had little effect on the transmission power.

3.2 Factor analysis for current of TX2 In the experiment of static situation, it can be seen that the voltage variation and minute current are flowing in TX2 for a very short time. In order to consider the cause, the simulation of the same situation was conducted. The simulation model is shown in Fig. 11.

The coil that controls power transmission is only TX1 connected to the u-phase and v-phase, and power transmission is not performed to TX2. As shown in Fig. 12, only the u and v phases send the gate drive signal, and the w phase is always in the gate off state.

The simulation results of stationary condition are shown in Fig. 13, Fig. 14. In the simulation model, the parasitic capacitance value of mosfet C_{ds} actually used in the experiment is included, and the value C_{ds} is 155 pF. For comparison, simulation was performed also when there was no parasitic capacitance (C_{ds} = 0). From the results of Fig. 13, it can be seen that only TX1 and RX can transmit power by WPT. The same waveform as in the experiment was seen in TX2. From the results of Fig. 14, due to the influence of parasitic capacitance, the voltage change of w-phase becomes slow, and a potential difference occurs in TX2 for a short time. This revealed that the parasitic capacitance was the cause of the voltage variation and minute current in TX2.

3.3 Experimental results of dynamic situation Fig. 15 shows the experimental waveform when two coils are operated with a three-phase inverter while moving the RX at 1 km/h. The distance between the two transmitter coils is set to 400 mm. This is a position where the mutual inductance between the transmitter coils is about 1/100 of the self-inductance, and its influence of mutual inductance between two transmitter coils is almost negligible. From the experimental results, it can be confirmed that each coil can be driven independently and transmitted to the RX. For about 2.8 seconds from the start of power transmission, only her arm connected to the first power transmission coil TX1 is operated and driven. At this time, it can be seen that the current flows only in TX1 and almost no current flows in TX2. It can be confirmed that the current is flowing through the RX and the power is being received. After that, when the transmitter current reaches the end of the transmitter coil where the mutual inductance becomes small, it can be confirmed that the current value increases. In this experiment, the current threshold was set to 4 A, therefore all gates were turned off when the current exceeded the threshold. The control cycle is 10 µs, then the control is performed in a sufficiently short

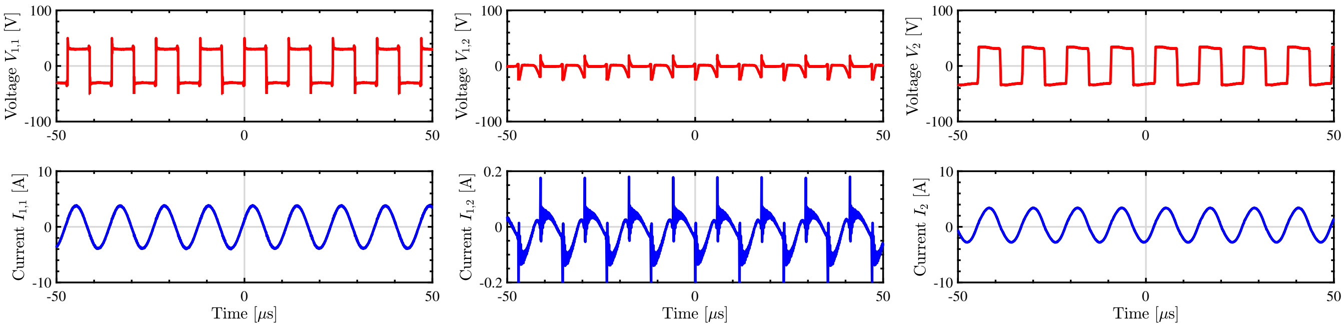

(a) TX1. (b) TX2. (c) RX.

Fig. 9. Experimental static current and voltage output waveform with two coils and one three-phase inverter.

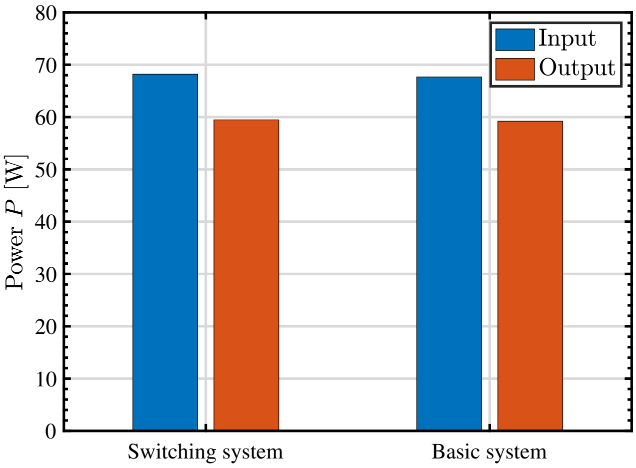

Fig. 10. Experimental result of input and output DC power with the switching and basic system(blue one is input power, red one is output power).

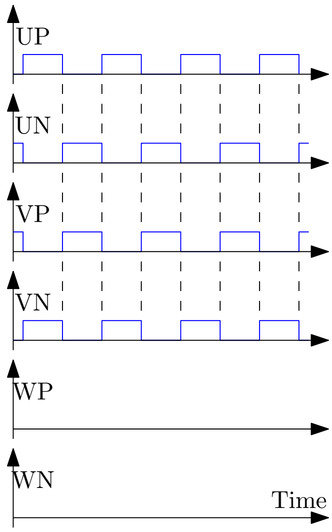

Fig. 12. Gate signal of simulation.

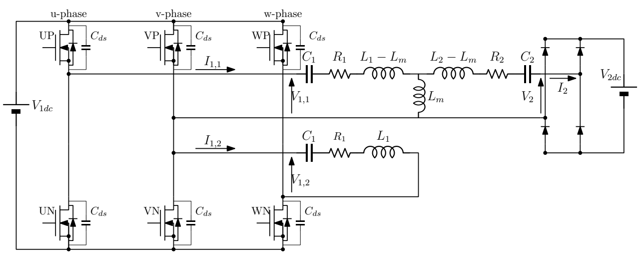

Fig. 11. Simulation model of the developed system.

Table 4. Experimental condition of dynamic situation.

Input voltage V_{1dc}	30 V
Output voltage V_{2dc}	30 V
frequency f_0	85 kHz
Velocity of Receiver coil	1 km/h
Threshold current I_{1th}	4 A
Gap of transmitter coil	400 mm

time compared to the time required to move in the power transmission section.

4. Conclusion

This paper discusses the coil switching system with a N-phase inverter configuration and control method that can independently drive multiple coils in the DWPT system. According to the coil switching system, multiple coils can be operated with a N-phase inverter that reduce the number of switching elements. The feasibility and fundamental opration was shown by simulation and experiment. Simulations and experiments revealed that a small amount of current flows through the coil that does not transmit power, but the results show that the amount and effciency of power supply is almost the same as that of the previous system. In addition, an experiment simulating DWPT was actually conducted, and it was demonstrated that control corresponding to changes in mutual inductance is also possible. In the future work, a five-phase or nine-phase inverter will be verified that the coil switching is possible as well. In addition, the introduction of vehicle detection technology using the method discussed in [11] will be considered.

Acknowledgment

This work was partly supported by JSPS KAKENHI (Grant Number JP18H03768) and JST-Mirai Program (Grant Number JPMJMI17EM).

References

(1) G. A. Covic and J. T. Boys, "Modern trends in inductive power transfer for transportation applications," *IEEE Journal of Emerging and Selected Topics in Power Electronics*, vol. 1, no. 1, pp. 28–41, 2013.

(2) O. Shimizu, S. Nagai, T. Fujita, and H. Fujimoto, "Potential for CO2 Reduction by Dynamic Wireless Power Transfer for Passenger Vehicles in Japan," *Energies*, vol. 13, no. 13, p. 3342, 2020.

(3) A. Kurs, A. Karalis, R. Moffatt, J. D. Joannopoulos, P. Fisher, and M. Sol-

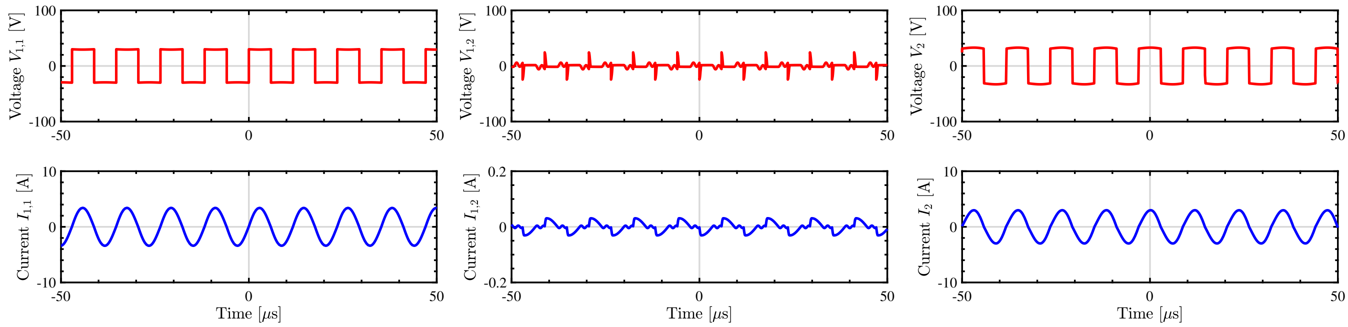

(a) TX1. (b) TX2. (c) RX.

Fig. 13. Simulational static current and voltage output waveform with two coils and one three-phase inverter($C_{ds} = 155 \times 10^{-12}$).

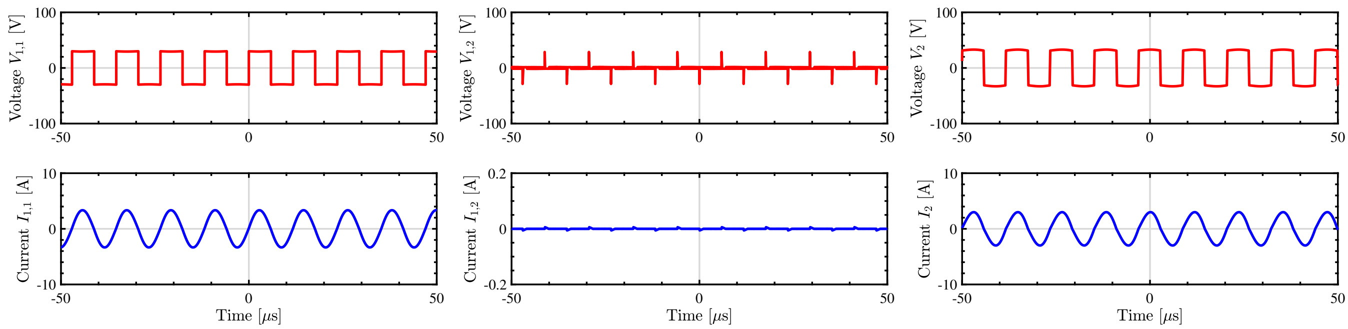

(a) TX1. (b) TX2. (c) RX.

Fig. 14. Simulational static current and voltage output waveform with two coils and one three-phase inverter($C_{ds} = 0$).

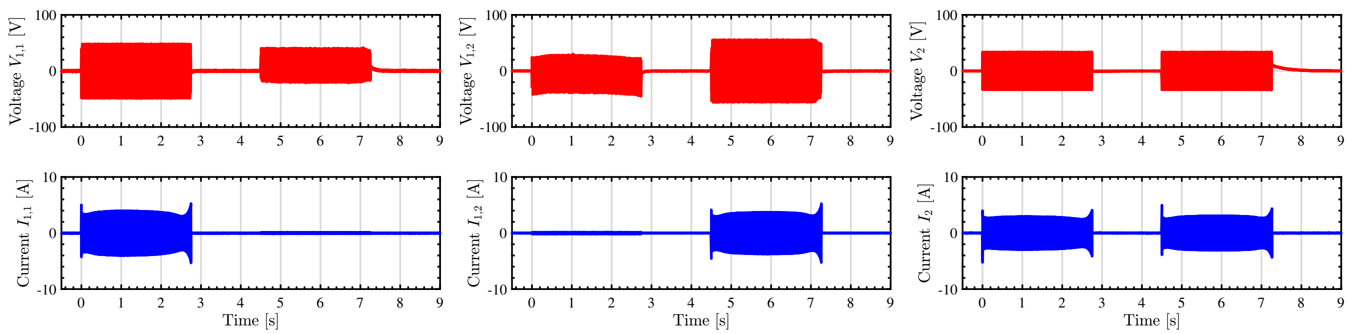

(a) TX1. (b) TX2. (c) RX.

Fig. 15. Experimental dynamic current and voltage output waveform with two coils and one three-phase inverter.

jacic, "Wireless Power Transfer via Strongly Coupled Magnetic Resonances," *Science*, vol. 317, no. 5834, pp. 83–86, jul 2007.

(4) T. Imura and Y. Hori, "Unified Theory of Electromagnetic Induction and Magnetic Resonant Coupling," *IEEJ Transactions on Industry Applications*, vol. 135, no. 6, pp. 697–710, 2015.

(5) A. Ahmad, M. S. Alam, and R. Chabaan, "A Comprehensive Review of Wireless Charging Technologies for Electric Vehicles," *IEEE Transactions on Transportation Electrification*, vol. 4, no. 1, pp. 38–63, mar 2018.

(6) T. Fujita, T. Yasuda, and H. Akagi, "A Dynamic Wireless Power Transfer System Applicable to a Stationary System," *IEEE Transactions on Industry Applications*, vol. 53, no. 4, pp. 3748–3757, 2017.

(7) H. Fujimoto, O. Shimizu, S. Nagai, T. Fujita, D. Gunji, and Y. Ohmori, "Development of Wireless In-wheel Motors for Dynamic Charging," *2020 IEEE PELS Workshop on Emerging Technologies: Wireless Power Transfer (WoW)*, pp. 56–61, 2020.

(8) J. Shin, S. Shin, Y. Kim, S. Ahn, S. Lee, G. Jung, S. J. Jeon, and D. H. Cho, "Design and implementation of shaped magnetic-resonance-based wireless power transfer system for roadway-powered moving electric vehicles," *IEEE Transactions on Industrial Electronics*, vol. 61, no. 3, pp. 1179–1192, 2014.

(9) V. Z. Barsari, D. J. Thrimawithana, and G. A. Covic, "Push-pull driven Low-cost Coupler Array for Dynamic IPT systems," pp. 209–213, 2020.

(10) K. Hata, T. Imura, and Y. Hori, "Proposal of Classification and Design Strategies for Wireless Power Transfer Based on Specification of Transmitter-Side and Receiver-Side Voltages and Power Requirements," *IEEJ Transactions on Industry Applications*, vol. 138, no. 4, pp. 330–339, 2018.

(11) H. Y. Kobayashi Daita, Imura Takehiro, "Sensorless Transmitting ON/OFF Switching System in Dynamic Wireless Power Transfer for Electric Vehicles," *13th ITS Symposium 2015*, 2015.